Numerical Assessment of EMF Exposure of a Cow to a Wireless Power Transfer System for Dairy Cattle

Said Benaissa[a, b,*], Amine M. Samoudi[a], David Plets[a], Günter Vermeeren[a], Leen Verloock[a], Ben Minnaert[c], Nobby Stevens[c], Luc Martens[a], Frank A.M. Tuyttens [b, d], Bart Sonck[b, e], Wout Joseph[a]

[a] Department of Information Technology, Ghent University/imec, Technologiepark-Zwijnaarde 15, 9052 Ghent, Belgium

[b] Flanders Research Institute for Agriculture, Fisheries and Food (ILVO). Animal Sciences Unit, Scheldeweg 68, 9090 Melle, Belgium

[c]Faculty of Engineering Technology, DraMCo Research Group, ESAT, KU Leuven, Ghent, Belgium

[d]Department of Nutrition, Genetics and Ethology, Faculty of Veterinary Medicine, Heidestraat 19, B-9820 Merelbeke, Belgium

[e]Department of Animal production, Faculty of Bioscience Engineering, Ghent University, Coupure links 653, B-9000 Ghent, Belgium

*** Corresponding author: Said Benaissa, Tel.: +32 09 331 48 60; E-mail address: said.benaissa@ugent.be**

Abstract

In this paper, we assessed the exposure of a cow to the electromagnetic fields (EMFs) induced by a wireless power transfer (WPT) system working at 92 kHz in a dairy barn. Cow exposure to the radiated EMFs was evaluated and compared to safety guidelines. We modeled a realistic WPT system for dairy cows in Sim4Life, a 3D electromagnetic simulation tool. We validated the model with electric field measurements; simulated fields deviated on average 6% from measured fields. We used the proposed WPT model to evaluate the stimulation and thermal effects based on the internal electric field and the specific absorption rate (SAR), respectively. Results showed that the exposure mainly varied with the distance of the transmitter to the body: variation of 5 dB of the induced electric field when the transmitter was set at 20 cm and 10 cm from the body. The distance of the receiver to the body influenced the exposure less (10%). We also compared the exposure with the limits provided by the International Commission on Non-Ionizing Radiation Protection (ICNIRP). The internal electric fields were more conservative than SAR, which showed values far below exposure limits.

Keywords

Dairy health monitoring, precision livestock farming (PLF), wireless power transfer, electromagnetic exposure, induced electric field, specific absorption rate (SAR), internet-of-animals

1. Introduction

The continuous demand for increased production and the efforts for minimizing the environmental impact and saving costs make cattle monitoring using on-cow sensors widely adopted in today's dairy farms (Andersson et al., 2016; Benaissa et al., 2016a, 2016b; González et al., 2015; Neethirajan, 2017; Rutten et al., 2017; Van Nuffel et al., 2015). As sensor nodes are generally battery-powered devices with low processing and storage capabilities, the critical aspects to face are how to increase the battery capacity, reduce the energy consumption of nodes and avoid frequent battery replacement. Energy harvesting methods for wearable devices have emerged as an attractive solution to overcome the power consumption challenges (Minnaert et al., 2017). Energy could be harvested using passive sources from motion and vibration, solar energy, and ambient radio frequency (RF) energy (Bhatnagar and Owende, 2015). Although the sources are often available, the amount of power harvested is in the micro-watt range, which is insufficient to operate RF wireless transceiver modules in wearable devices (Nguyen et al., 2015). On the other hand, active energy sources involve wireless power transmission (WPT) coils to supply power to wearable devices. WPT can be conveniently optimized to satisfy power supply requirements. Moreover, WPT facilitates long term cow monitoring, as it allows an easy optimization of power supply, eliminates frequent battery replacement and reduces the weight and size of the wearable sensor (Minnaert et al., 2017).

However, the integration of WPT components would generate electromagnetic fields (EMF) in the proximity of the cow. Therefore, it is necessary to characterize EMF induced in the cow's body by a WPT system in a dairy barn. Effects of other EMF sources on cows (i.e., RF, stray voltage, extremely low frequency (ELF) electric and magnetic fields) have been frequently discussed in journals and meetings with agricultural, veterinary or dairy backgrounds (Algers and Hultgren, 1987; Burchard et al., 1998; Burda et al., 2009; Hillman et al., 2013). For instance, Löscher (2003) reported that dairy cows exposed to TV and radio transmitting antennas showed reduced milk yield, health problems (e.g.

avoidance behavior, poor general condition), and behavioral abnormalities (Löscher, 2003). In addition, Erdreich et al. (2009) did not observe any indications that bovine production and behavior were affected by exposure to up to 3 mA of stray voltage at 50 or 60 Hz for up to 3 or 4 weeks. However, Hillman et al. (2013) found that not only the cows´ behavior, but also health and milk production were negatively affected by stray voltage fields. Moreover, Burchard et al. (1998) concluded that exposure to ELF EMF (i.e., 60 Hz, 10 kV/m, 30 µT) for several 28-day-periods had no effects on cow progesterone levels. Although, the exposed animals had a prolonged estrous cycle.

None of these studies has provided numerical or experimental estimates of cow exposure to EMF. Also, no work has investigated the electromagnetic effect of WPT system on the cow's body. Therefore, the aim of this work was to numerically model a realistic WPT system for dairy cows using a 3-D electromagnetic solver (Sim4Life), to validate the proposed model with experiments, to assess the cow's exposure to the radiated EMF by calculating the internal electric field and the SAR, and to compare the results with the safety exposure guidelines. We compared cow exposure to EMF with guidelines for human exposure, as, to date, no guidelines exist for animal exposure to EMF. For human exposure, international bodies like the International Commission on Non-Ionizing Radiation Protection (ICNIRP, 2010) and the Institute of Electrical and Electronics Engineers (IEEE, 2006) provide guidelines to limit the human exposure to time-varying electric, magnetic and electromagnetic field (ICNIRP, 2010; IEEE, 2006).

2. WPT system for dairy cows

We tested the WPT system presented by Minnaert et al., (2017) at the Flanders Research Institute for Agriculture, Fisheries and Food (ILVO) in Melle, Belgium. Fig. 1-a shows a cow in the feeding trough where the WPT system was installed. When the cow was eating, the transmitter located at the feeding trough transmitted energy to the receiver attached to the collar of the cow. The transmitter coil (Fig. 1-b) had an oval shape of 27.0 cm x 13.5 cm and was installed on a 32.5 cm x 15.6 cm x 0.6 cm layer of ferrite (3F4). The receiver coil (Fig.1-c) had an oval shape of 12.6 cm x 9.6 cm with a

6.5 cm x 5.2 cm x 0.6 cm ferrite core. Both coils had 5 turns made of 1.5 mm² Cu wire. The optimal dimensions of the coils were experimentally determined for a maximum power transfer. The resonance frequency was 92 kHz. The electrical parameters of the TX and RX coils measured with an Agilent 4285A LCR meter at 92 kHz are listed in Table 1. More details about the system are available in Minnaert et al., (2017).

3. Materials and Methods

3.1 Computational techniques and Quasi-Static (QS) approximation

In this study, the 3-D electromagnetic solver Sim4Life (Maiques, 2014) was used. For frequencies above 1 MHz, simulations were performed with the finite difference time domain (FDTD) method; for frequencies below 1 MHz, the quasi-static (QS) approximation using the finite element method (FEM) was employed to reduce the computational complexity and the simulation time (Laakso et al., 2015; Samoudi et al., 2016). The applicability of the QS approximation has been proven for human exposure to WPT systems for frequencies up to 10 MHz by Laakso et al. (2015).

Instead of using a one-step method based on a full-wave analysis for the original problem all at once, a two-step process was used as explained in Park and Kim (2016). Using this method, the number of time steps can be considerably decreased due to rapid convergence within a time shorter than one full period, whereas the conventional method has to simulate several periods to reach the steady state. The first step is to obtain the EMFs generated from the WPT system in the absence of the cow's body. In the second step, the induced EMFs in the cow's body is calculated with a QS-FEM method by regarding the EMFs obtained in the previous step as the incident field to the cow's body.

3.2 Electromagnetic modeling of the WPT system and cow's body

3.2.1 Modeling of the WPT system

Fig. 2 shows the transmitter and the receiver coils of the WPT system as modelled in Sim4Life. Both coils were modelled with five turns of a prefect conductive 1.5 mm^2 wire. The transmitter coil was installed on a rectangular ferrite (Fig. 2-a), while the receiver coil has a core ferrite with the same

dimensions as the experimental coil. The relative permeability of the ferrite (i.e., 3F4) is 900 at 92 kHz (Matz et al., 2009).

3.2.2 Modelling of the cow's body

We used the homogeneous cow model developed by Benaissa et al. (2016b); for human body simulations, several anatomical models are available (Ackerman, 1998), , but no anatomical models exist for a cow's body. The cow's body was modelled as a homogeneous medium with the following dimensions: withers-tail 1.8 m, width 0.7 m, nose-tail 2.6 m, rump-hoof 1.4 m, stance (i.e., front-to-rear claws) 1.7 m, chest 0.8 m, withers (shoulder) height 1.4 m, and hook-bone width 0.6 m (Benaissa et al., 2016b). The numerical cow model is composed of muscle tissue with the dielectric properties at the operating frequency of the system (92 kHz); conductivity σ=0.35 S/m and relative permittivity ε_r=8097 (Gabriel et al., 1996). Uniform rectilinear meshes were applied to easily discretize the complex anatomical models with a voxel size of 2 mm along x, y, and z direction.

3.3 Experimental setup for the validation of the WPT system

To validate the numerical model of the WPT system, we compared simulated free-space magnetic fields emitted by the WPT system with the measured fields. The peak value of the magnetic field was measured with the EHP-50 electric and magnetic field probe (Narda safety test solutions, Milan, Italy). The isotropy error of this probe for the magnetic field is ±0.8 dB at 1 MHz and its frequency response is ±0.8 dB over a frequency range from 9 kHz to 30 MHz. Field sensors (radius 46 mm) and electronic measuring circuitry were fitted into a housing of 92 x 92 x 109 mm^3 in size. The probe was mounted on a plastic mast at 1 m above the ground as shown in Fig. 3-a. We, first, measured without the receiver coil as shown in Fig. 3-b. The transmitter was kept in a fixed position. Then, the field analyzer was positioned at different distances from the TX coil (i.e., 2, 5, 10, 15, 20 cm). The center point of the probe was aligned with the horizontal axis of the coil. Next, we measured with both transmitter and receiver. In this case, the H-field was measured 5 cm from the RX coil for different TX-RX separations (i.e., 10, 15, 20 cm) as shown in Fig. 3-c. The E-field was not considered in the validation since the dominant coupling with the body is due to the magnetic field (Kuster and Balzano, 1992).

The transmitter was powered by a DC supply with a DC voltage of 12.00 V and a DC current of 305 mA, corresponding with an active input power of 3.66 W. This input power was converted with an efficiency of 27.3 % to a transmitting power of 1.0 W at the transmitter coil. The peak voltage and current in the transmitter coil were 42.0 V and 6.32 A, respectively. The AC power received at the receiver coil is given in the Table 2, as well as the coupling factors for the different distances. Peak voltage and current in the receiver coil at 10 cm distance were 7.5 V and 2.9 A, respectively. For the simulations, a current of 7.5 A (peak value) was applied to the TX coil. The received current at the RX coil as well as the coupling factor could not be calculated by the simulator.

3.4 Exposure scenarios

To mimic realistic exposure scenarios, the WPT system was located at different distances below the cow's neck. Experiments in Minnaert et al., (2017) showed that the distance between the receiver coil and the cow's neck could vary from 2 cm up to 5 cm, whereas the distance between the transmitter coil and the cow's neck could vary from 10 cm up to 20 cm. Therefore, the RX and TX in the simulations were set at d1 (2.5 and 5 cm) and d2 (10, 15, and 20 cm), respectively, from the cow's body (Fig. 4). The values of d1 and d2 for each scenario are listed in Table 3.

3.5 ICNIRP and IEEE fields evaluation and limits

As guidelines for animal exposure to EMF lack, guidelines for human exposure were used in this study. The guidelines protect against stimulation effects for frequencies up to 10 MHz and protect against thermal effects for frequencies between 100 kHz and 10 GHz. Protection against stimulation effects is in terms of the 99th percentile of the internal electric field; protection against thermal effects is in terms of the specific absorption rate (SAR). Since the operating frequency of the WPT system is around 100 kHz, both the internal electric field and the SAR were considered in this study. The compliance of the WPT system with international EMF exposure guidelines was investigated using the parameters from these standards. ICNIRP 2010 (ICNIRP, 2010) calculates the induced electric field as a vector average within a contiguous tissue cubic volume of 2×2×2 mm^3. It suggests using the 99th percentile value of the calculated internal electric field for the compliance with the guidelines. However, in the

IEEE standard (IEEE, 2006), the internal electric field is specified as an arithmetic average of electric fields projected onto a straight line segment of 5 mm length oriented in any direction within the tissue. We note that for IEEE standard, the exposure limits for uncontrolled environments were considered.

4. Results

4.1 WPT system validation

Fig. 5 shows the measured and the simulated H-fields for the TX coil alone case (Fig.3 –b). For all cases (middle, right, and left sides), agreement between the measurements and simulations was achieved, especially for distances greater than 5 cm from the TX coil. At 2 cm, the probe is close to the wires of the coils, which could influence the field generated by the coil. Table 4 lists the measured and simulated H-field for the full WPT system (Fig. 3-c). Also in this case, the results show good agreement between the measurements and simulations with differences less than 2 A/m.

The maximum, the minimum, and the average of the relative and absolute errors between the measured and simulated H-field samples are listed in Table 5. The relative error varies between 2.25 % and 9.92 % with an average of 5.87 % and the absolute error varies between 0.07 A/m and 7.95 A/m with an average of 1.67 A/m. The maximum errors occurred in close proximity of the coils (2 cm); however, the average relative error was less than 6 %.

4.2 E-field distribution

Fig. 6 shows the internal electric field (in dB normalized to 0.5 V/m) in the cow for all investigated scenarios (Section 3.4) for an input power of 1 W. Scenario I showed the largest internal electric fields (0.49 V/m), whereas scenario VI showed the minimum values (0.11 V/m). This is due to the configuration of the TX coil playing the major role in the electric field induction in the cow. In scenario I, the TX is at its nearest location to the cow neck while it is at its furthest position from the cow in scenario VI. The distance between RX coil and the cow did not have much effect on the induced electric field (differences less than 10%), when the TX coil was at a fixed distance from the cow's body.

4.3 E_{max} and $E_{99\%}$ for ICNIRP 2010 and IEEE 2005

In order to study the coils compliance with the basic restrictions (ICNIRP, 2010; IEEE, 2006), the internal induced electric fields were calculated using the maximum value and the 99th percentile value. ICNIRP 2010 recommends a maximum value of 13.5 V/m for internal E-field at 92 kHz, while the IEEE guidelines recommend a maximum of 20.9 V/m for internal E-field. Table 6 lists the calculated electric field in the cow model for the considered scenarios. The highest induced electric field (Table 6) occurs for the scenarios I and IV (maximum $E_{99\%}$ of 0.21 V/m and 0.20 V/m for I and IV, respectively). For these scenarios, the distance d2 is at its minimum (d2=10 cm) making the TX coil at the nearest position to the cow. The lowest $E_{99\%}$ (0.066 V/m) occurred when both the TX and RX are at the furthest position from the cow (d1 = 5 cm and d2 = 20 cm). A 3.5 % difference between scenarios I and IV (changing only the RX position) compared to a 48.5 % difference between scenarios I and II (changing only the TX position) shows that TX coil has the greater effect on the $E_{99\%}$ compared to the RX coil. The great effect of the TX coil on the induced electric field was also reported and discussed in section 4.2. For an input power of 1 W, the limits were not exceeded for both ICNIRP and IEEE guidelines.

4.4 Local and whole-body SAR

To investigate the thermal effect of the WPT system and its compliance with ICNIRP and IEEE guidelines, the peak localized SAR (SAR_{1g} and SAR_{10g}) and whole-body SAR (SAR_{wb}) were computed for the six exposure scenarios defined in section 3.4. Table 7 lists the obtained values for an input power of 1 W. The induced whole-body SAR values vary between 7.11 µW/kg (Scenario I) and 0.39 µW/kg (scenario VI). For the local SAR (SAR_{1g} and SAR_{10g}), the obtained values were higher than the whole-body SAR values. SAR_{10g} varied between 44.63 µW/kg (scenario I) and 2.58 µW/kg (scenario VI). Similarly, SAR_{10g} varied between 56.76 µW/kg and 3.12 µW/kg. Similar to what was found for the electric field, the TX coil has a greater effect on the SAR values than the RX coil.

5. Discussion

This work is a first step to study the exposure of the cow's body to WPT systems. After the validation of the experimental WPT system, the induced electric field and the SAR values were computed based

on Sim4Life simulations for different separations between the source (transmitter and receiver coils) and the cow's body. The induced electric field depended mainly on the distance between the transmitter and the cow's body, with variations exceeding 5 dB between scenario I and scenario VI. However, the distance between the receiver and the cow's body had less influence (10%). In comparison to human exposure limits (13.5 V/m for ICNIRP 2010 and 20.9 V/m for IEEE 2006), the induced electric field values were lower than the limits for all the investigated scenarios. This could be explained by the low input power used for the simulations. To deploy the WPT system in barns, the values of the induced electric field computed in this paper could be used to derive the maximum allowable input power that has to be respected to stay under the exposure limit. For the SAR, the obtained values were lower than 1% of the limit (0.08 for SAR_{wb}, 1.6 W/kg for SAR_{1g} and 2 W/kg for SAR_{10g}). This means that the thermal effect of the WPT system is very limited at that frequency (92 kHz). This is because the operating frequency is slightly below 100 kHz. Therefore, the maximum allowable transmit power at which the SAR limit is reached is in the order of several kW, which is in our case, far above the range of input power used in wireless power transfer system in a dairy barn (in W). Above 100 kHz, ICNIRP specifies its basic restriction to prevent whole-body heat stress and excessive localized tissue heating in terms of SAR. Therefore, the induced electric field restriction is the most stringent exposure limit for the evaluation of the WPT coils. The same conclusions were drawn in (Park, 2017) about human exposure to WPT systems. In that work, SAR_{wb} values between 0.15 and 1.31 µW/kg were reported for an input power of 1 W. As stated in the IEEE C95.1-2005 standard (IEEE, 2006), guidelines (IEEE and ICNIRP) provide recommendations to minimize aversive or painful electrostimulation in the frequency range of 3 kHz to 5 MHz and to protect against adverse heating in the frequency range of 100 kHz to 300 GHz. Below 100 kHz, the aversive or painful electrostimulation is the effect being minimized. At low frequencies, exposures are assessed in terms of instantaneous fields or currents (internal electric field used in our study). Above 100 kHz, there can be a sensation of heat, which is not considered adverse. Above 100 kHz, exposures are assessed with reference to an average time that varies with frequency (SAR used in our study). The frequency of 100 kHz nominally

represents a “thermal crossover” below which electrostimulation effects dominate, and above which thermal effects dominate for continuous wave exposure (IEEE, 2006). This justifies why the SAR values, mainly used to minimize adverse heating effects, are negligible compared to the limits for the considered system (lower than 1% of the limit). SAR values will be much higher (compared to limits) in the MHz range, and the opposite will happen for the internal electric field.

The homogeneous body of the cow phantom was one limitation of the present study. A heterogeneous model - including other tissues than muscle only- will give more realistic values for the exposure metrics. Also, this study considers only the case when the centres of the transmitter and receiver coil are perfectly aligned (i.e., optimal power transfer). When the coils are misaligned, either laterally or angularly, the magnetic flux through the receiver coil will decrease, leading to a lower power transfer (Fotopoulou and Flynn, 2011). However, this may increase the SAR values as reported in (Park, 2017) The analysis performed in that work showed that the worst-case exposure scenario (higher values of the SAR) generally occurred in the misalignment case. Therefore, further research is required in this direction.

6. Conclusions and future work

In this paper, we investigated cow exposure to EMF of a WPT system operating at 92 kHz. After the experimental validation of the WPT source, the induce fields in the cow’s body were numerically computed using 3-D electromagnetic software (Sim4Life). Cow exposure dependents mainly on the separation between the transmitter and cow’s body; the distance between the receiver and the cow’s body has less influence (10%) on the exposure metrics. We also observed that, unlike the stimulation effect, the thermal effect, evaluated by the specific absorption rate, of the WPT system on the cow’s body is very limited. Therefore, the induced electric field will mainly define the final acceptable input power level. In future works, the effect of the cow’s body posture, the inner anatomy (i.e., heterogeneous phantom), and off-centering effect of the coils should be taken in consideration. Also, the WPT systems operating in the MHz range should be investigated, since the stimulation effect does

not occur in this range. Finally, the influence of the exposure to the cows' behavior (i.e., feeding) and production (i.e., milk) should be investigated. This is a mandatory step before integrating the system in the dairy farm.

7. Acknowledgments

This work was executed within MoniCow, a research project bringing together academic researchers and industry partners. The MoniCow project was co-financed by imec (iMinds) and received project support from Flanders Innovation & Entrepreneurship.

8. References

Ackerman, M.J., 1998. The visible human Project: A resource for anatomical visualization, in: Studies in Health Technology and Informatics. pp. 1030–1032. doi:10.3233/978-1-60750-896-0-1030

Algers, B., Hultgren, J., 1987. Effects of long-term exposure to a 400-kV, 50-Hz transmission line on estrous and fertility in cows. Prev. Vet. Med. 5, 21–36. doi:10.1016/0167-5877(87)90003-1

Andersson, L.M., Okada, H., Miura, R., Zhang, Y., Yoshioka, K., Aso, H., Itoh, T., 2016. Wearable wireless estrus detection sensor for cows. Comput. Electron. Agric. 127, 101–108. doi:10.1016/j.compag.2016.06.007

Benaissa, S., Plets, D., Tanghe, E., Verloock, L., Martens, L., Hoebeke, J., Sonck, B., Tuyttens, F.A.M., Vandaele, L., Stevens, N., Joseph, W., 2016a. Experimental characterisation of the off-body wireless channel at 2.4GHz for dairy cows in barns and pastures. Comput. Electron. Agric. 127, 593–605. doi:10.1016/j.compag.2016.07.026

Benaissa, S., Plets, D., Tanghe, E., Vermeeren, G., Martens, L., Sonck, B., Tuyttens, F.A.M., Vandaele, L., Hoebeke, J., Stevens, N., Joseph, W., 2016b. Characterization of the on-body path loss at 2.45 GHz and energy efficient WBAN design for dairy cows. IEEE Trans. Antennas Propag. 11, 4848–4858. doi:10.1109/TAP.2016.2606571

Bhatnagar, V., Owende, P., 2015. Energy harvesting for assistive and mobile applications. Energy Sci. Eng. doi:10.1002/ese3.63

Burchard, J.F., Nguyen, D.H., Block, E., 1998. Progesterone concentrations during estrous cycle of dairy cows exposed to electric and magnetic fields. Bioelectromagnetics 19, 438–43.

Burda, H., Begall, S., Cerveny, J., Neef, J., Nemec, P., 2009. Extremely low-frequency electromagnetic fields disrupt magnetic alignment of ruminants. Proc. Natl. Acad. Sci. 106, 5708–5713. doi:10.1073/pnas.0811194106

Erdreich, L.S., Alexander, D.D., Wagner, M.E., Reinemann, D., 2009. Meta-analysis of stray voltage on dairy cattle. J. Dairy Sci. 92, 5951–5963. doi:10.3168/jds.2008-1979

Fotopoulou, K., Flynn, B.W., 2011. Wireless power transfer in loosely coupled links: Coil misalignment model. IEEE Trans. Magn. 47, 416–430. doi:10.1109/TMAG.2010.2093534

Gabriel, S., Lau, R.W., Gabriel, C., 1996. The dielectric properties of biological tissues: III. Parametric models for the dielectric spectrum of tissues. Phys. Med. Biol. 41, 2271–2293. doi:10.1088/0031-9155/41/11/003

González, L.A., Bishop-Hurley, G.J., Handcock, R.N., Crossman, C., 2015. Behavioral classification of data from collars containing motion sensors in grazing cattle. Comput. Electron. Agric. 110, 91–102. doi:10.1016/j.compag.2014.10.018

Hillman, D., Stetzer, D., Graham, M., Goeke, C.L., Mathson, K.E., Vanhorn, H.H., Wilcox, C.J., 2013. Relationship of electric power quality to milk production of dairy herds - field study with literature review. Sci. Total Environ. 447, 500–14. doi:10.1016/j.scitotenv.2012.12.089

ICNIRP, 2010. Guidelines for limiting exposure to time-varying electric and magnetic fields (1 Hz to 100 kHz). Health Phys. 99, 818–36. doi:10.1097/HP.0b013e3181f06c86

IEEE, 2006. IEEE Standard for Safety Levels With Respect to Human Exposure to Radio Frequency Electromagnetic Fields, 3 kHz to 300 GHz, IEEE Std C95.1-2005 (Revision of IEEE Std C95.1-1991). doi:10.1109/IEEESTD.2006.99501

Kuster, N., Balzano, Q., 1992. Energy Absorption Mechanism by Biological Bodies in the Near Field of Dipole Antennas Above 300 MHz. IEEE Trans. Veh. Technol. 41, 17–23. doi:10.1109/25.120141

Laakso, I., Shimamoto, T., Hirata, A., Feliziani, M., 2015. Quasistatic approximation for exposure assessment of wireless power transfer. IEICE Trans. Commun. E98B, 1156–1163. doi:10.1587/transcom.E98.B.1156

Löscher, W., 2003. Die auswirkungen elektromagnetischer felder von mobilfunksendeanlagen auf leistung, gesundheit und verhalten landwirtschaftlicher nutztiere: Eine bestandsaufnahme. Prakt. Tierarzt 84, 850–863.

Maiques, M.M., 2014. Sim4Life: A Simulation Platform for Life Sciences and Medtech Applications. Eur. Cells Mater. 27.

Matz, R., Gotsch, D., Karmazin, R., Manner, R., Siessegger, B., 2009. Low temperature cofirable MnZn ferrite for power electronic applications. J. Electroceramics 22, 209–215. doi:10.1007/s10832-007-9334-9

Minnaert, B., Thoen, B., Plets, D., Joseph, W., Stevens, N., 2017. Optimal energy storage solution for

319 an inductively powered system for dairy cows, in: WPTC 2017 - Wireless Power Transfer
320 Conference. doi:10.1109/WPT.2017.7953805

321 Neethirajan, S., 2017. Recent advances in wearable sensors for animal health management. Sens.
322 Bio-Sensing Res. doi:10.1016/j.sbsr.2016.11.004

323 Nguyen, C.M., Kota, P.K., Nguyen, M.Q., Dubey, S., Rao, S., Mays, J., Chiao, J.C., 2015. Wireless power
324 transfer for autonomous wearable neurotransmitter sensors. Sensors (Switzerland) 15, 24553–
325 24572. doi:10.3390/s150924553

326 Park, S., Kim, M., 2016. Numerical Exposure Assessment Method for Low Frequency Range and
327 Application to Wireless Power Transfer. PLoS One 11. doi:ARTN
328 e016672010.1371/journal.pone.0166720

329 Park, S.W., 2017. Misaligned Effect and Exposure Assessment for Wireless Power Transfer System
330 Using the Anatomical Whole-Body Human Model 77, 19–28.

331 Rutten, C.J., Kamphuis, C., Hogeveen, H., Huijps, K., Nielen, M., Steeneveld, W., 2017. Sensor data on
332 cow activity, rumination, and ear temperature improve prediction of the start of calving in dairy
333 cows. Comput. Electron. Agric. 132, 108–118. doi:10.1016/j.compag.2016.11.009

334 Samoudi, A.M., Vermeeren, G., Tanghe, E., Van Holen, R., Martens, L., Josephs, W., 2016. Numerically
335 simulated exposure of children and adults to pulsed gradient fields in MRI. J. Magn. Reson.
336 Imaging 44, 1360–1367. doi:10.1002/jmri.25257

337 Van Nuffel, A., Zwertvaegher, I., Van Weyenberg, S., Pastell, M., Thorup, V.M., Bahr, C., Sonck, B.,
338 Saeys, W., 2015. Lameness detection in dairy cows: Part 2. Use of sensors to automatically
339 register changes in locomotion or behavior. Animals. doi:10.3390/ani5030388

340

9. Figure captions

Fig. 1. A cow in the feeding trough where the WPT is installed (a). When the cow is feeding, the transmitter coil (b) transmits energy to the receiver coil (c).

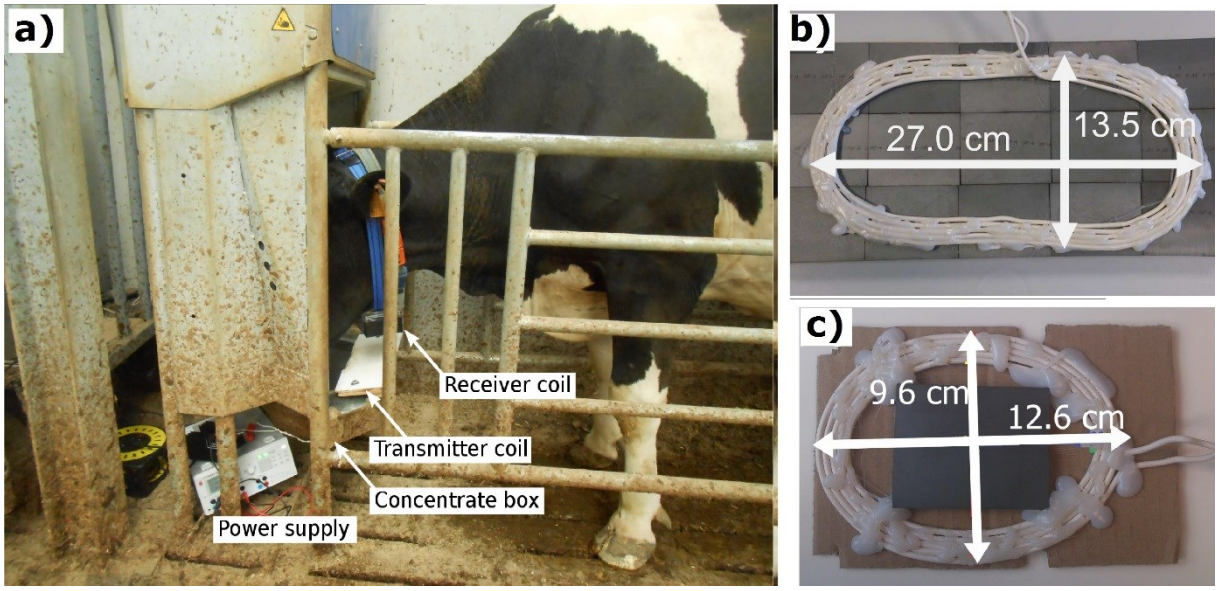

Fig. 2. Numerical model of the WPT system in the simulation software Sim4Life. Transmitter (a), receiver (b). The transmitter coil was installed on a 32.5 cm x 15.6 cm x 0.6 cm layer of ferrite and the receiver coil had a 6.5 cm x 5.2 cm x 0.6 cm ferrite core.

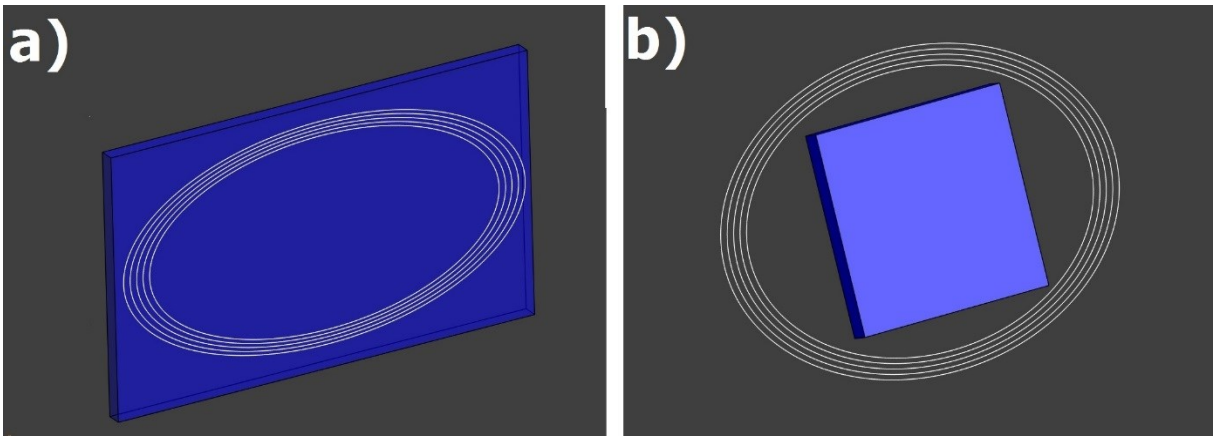

Fig. 3. Experimental setup for the validation of the numerical WPT model (a). The H-field was measured and calculated at different positions with TX alone (b) and TX and RX together (c).

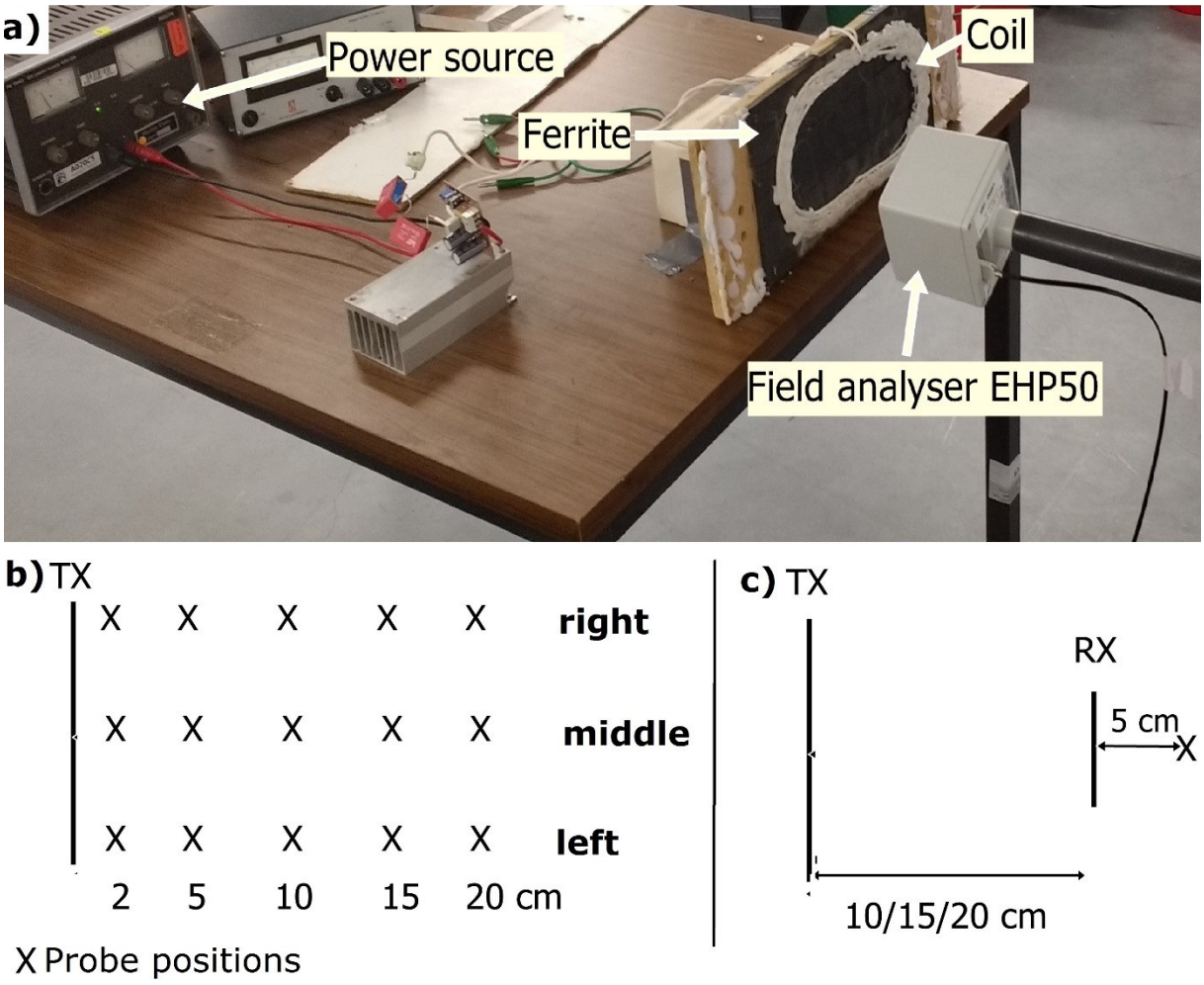

355 **Fig. 4.** Exposure scenarios: the RX and TX were set at d1 (2.5 and 5 cm) and d2 (10, 15, and 20 cm),
356 respectively, from the cow's body.

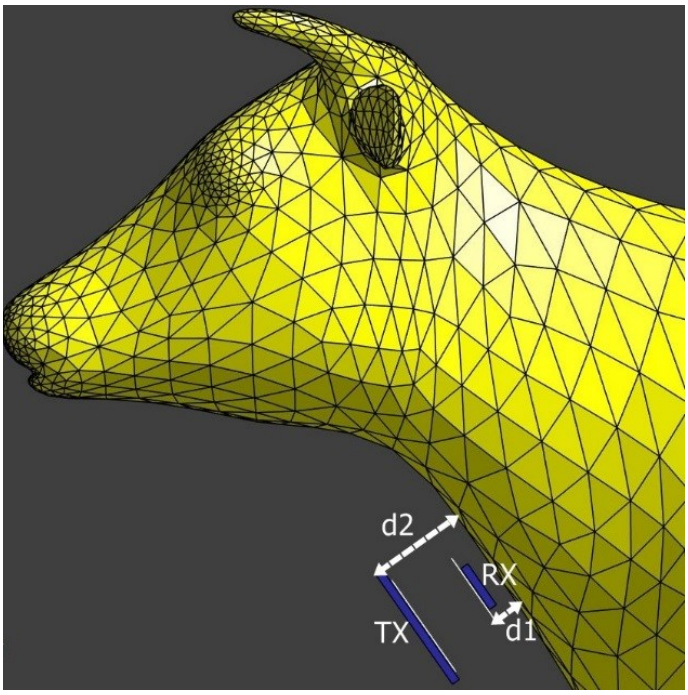

357

358

Fig. 5. Simulated and measured H-field values from the TX coil alone in the middle and in the left and right sides of the horizontal axis. (Middle, left, and right are defined in Fig. 3-b).

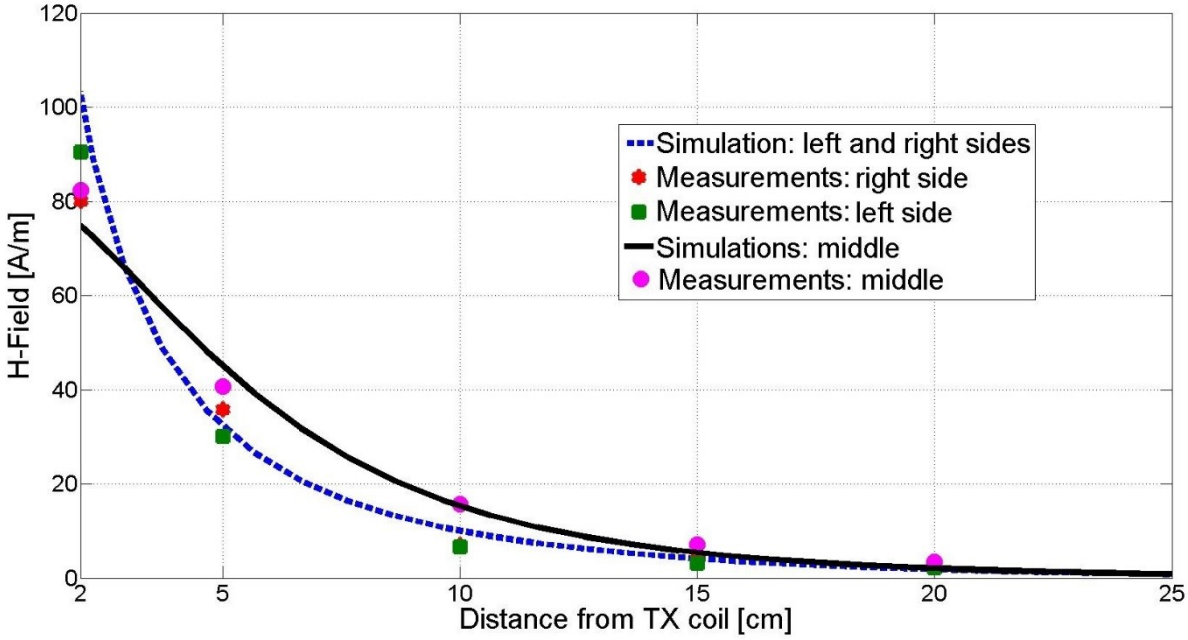

Fig. 6. Distribution of the internal electric field in the cow's body for the six scenarios defined in Table 3 for an input current (peak) of 7.5 A (input power of 1 W). The lines under the cow's neck are the transmitter and the receiver of the WPT system.

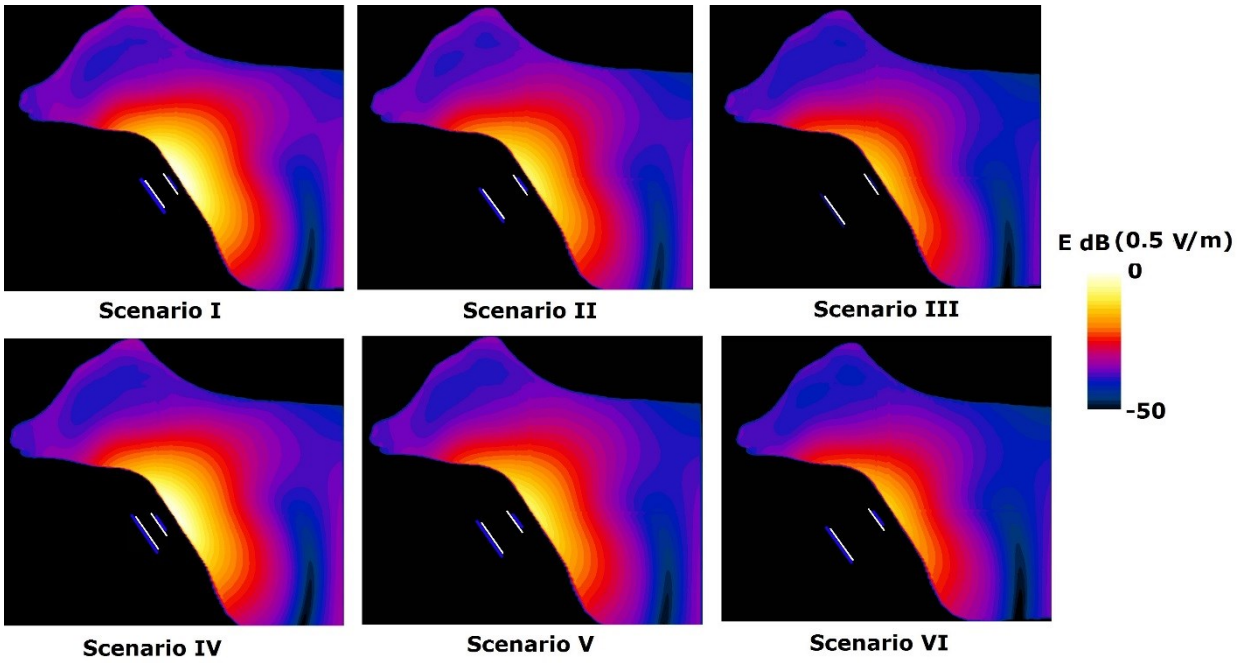

10. Table captions

	Transmitter coil (TX)	Receiver coil (RX)
Inductance L	15 µH	4.71 µH
Quality factor Q	170	53
Resistance R	0.05 Ω	0.05 Ω

Table 1. The electrical parameters of the TX and RX coils measured with an Agilent 4285A LCR meter at 92 kHz.

Distance TX-RX	Received power at the receiver coil	Magnetic link efficiency coil to coil.	Coupling factor k
10 cm	430 mW	43.0 %	4.8%
15 cm	185 mW	18.5 %	2.7%
20 cm	35 mW	3.5 %	1.3%

Table 2. The measured AC power received at the receiver coil for each TX-RX separation

		Distance d2 [cm]		
		10	15	20
Distance d1 [cm]	2.5	Scenario I	Scenario II	Scenario III
	5	Scenario IV	Scenario V	Scenario VI

Table 3. The distances of the transmitter coil (d1) and the receiver coil (d2) above the cow's body for the investigated scenarios.

TX-RX separation [cm]	10	15	20
H- field Measurements [A/m]	24.96	10.91	5.06
H- field Simulations [A/m]	23.22	10.36	5.57

Table 4. Simulated and measured H-Field values for TX and RX together.

	Maximum	Minimum	Average
Relative error[1] [%]	9.92	2.25	5.87
Absolute error[2] [A/m]	7.95	0.07	1.64

Table 5. Simulation versus measurements relative and absolute errors

[1] Difference calculated as follows | (Simulation-Measurement)/ Simulation |*100.

[2] Error field calculated as follows |Simulation − Measurement |.

Scenarios	ICNIRP		IEEE	
	E_{max}(V/m)	$E_{99\%}$ (V/m)	E_{max}(V/m)	$E_{99\%}$ (V/m)
I (d1=2.5 cm, d2=10 cm)	0.491	0.208	0.466	0.208
II (d1=2.5, d2=15)	0.224	0.107	0.213	0.107
III (d1=2.5, d2=20)	0.112	0.072	0.108	0.072
IV (d1=5, d2=10)	0.445	0.201	0.433	0.201
V (d1=5, d2=15)	0.214	0.097	0.207	0.097
VI (d1=5, d2=20)	0.110	0.066	0.101	0.066

385 **Table 6**. E_{max} and $E_{99\%}$ of the simulated E-field distribution for an input current (peak) of 7.5 A

386 (input power of 1 W) for the six scenarios explained in Table 3.

387

Scenarios	SARwb (μW/kg)	SAR_{10g} (μW/kg)	SAR_{1g} (μW/kg)
I (d1=2.5 cm, d2=10 cm)	7.11	44.63	56.76
II (d1=2.5, d2=15)	2.65	9.87	12.34
III (d1=2.5, d2=20)	0.42	2.61	3.17
IV (d1=5, d2=10)	6.03	44.30	56.48
V (d1=5, d2=15)	1.53	9.77	12.22
VI (d1=5, d2=20)	0.39	2.58	3.12

388 **Table 7.** SAR statistics in (μW/kg) for an input current (peak) of 7.5 A (input power of 1 W) for the

389 six scenarios explained in Table 3.

390